

InAs/GaSb cascaded active region superlattice light emitting diodes for operation at 3.8 μm

E. J. Koerperick,^{1,2,3,a)} J. T. Olesberg,^{3,4} T. F. Boggess,^{1,2,3} J. L. Hicks,^{2,3} L. S. Wassink,^{2,3} L. M. Murray,^{2,3} and J. P. Prineas^{2,3}

¹Department of Electrical and Computer Engineering, University of Iowa, Iowa City, Iowa 52242, USA

²Department of Physics and Astronomy, University of Iowa, Iowa City, Iowa 52242, USA

³Optical Science and Technology Center, University of Iowa, Iowa City, Iowa 52242, USA

⁴Department of Chemistry, University of Iowa, Iowa City, Iowa 52242, USA

(Received 4 September 2007; accepted 15 February 2008; published online 26 March 2008)

We report on the growth and characterization of InAs/GaSb superlattice light emitting diodes (LEDs) operating in the midwave infrared at 3.8 μm at 77 K. Devices were grown by solid source molecular beam epitaxy on (100) GaSb substrates and were fabricated into $120 \times 120 \mu\text{m}^2$ mesa devices using wet etching. By employing an eight-stage cascaded active region design, output powers in excess of 1.5 mW were achieved at 77 K with 100 mA peak drive current and a 50% duty cycle. Operating characteristics of the devices were examined from room temperature to 77 K under quasi-dc excitation conditions. © 2008 American Institute of Physics. [DOI: 10.1063/1.2892633]

Modern epitaxial growth techniques have enabled the development of a vast array of semiconductor heterostructures that have applications in numerous fields of science and industry. The ability to tailor the compositional and doping profile of a semiconductor structure on a monolayer scale enables precise control of the optical and electronic properties of the material. Initially proposed by Esaki and Tsu,¹ compositional superlattices (SLs) consist of alternating layers of materials with thickness less than the electron de Broglie wavelength. This work utilizes the InAs/GaSb SL material system grown on GaSb substrates for fabrication of high output light emitting diodes (LEDs). SLs in this material system exhibit a type-II broken gap band alignment in which the electrons and holes are primarily localized in the InAs and GaSb layers, respectively. By properly choosing the layer thickness, the energy gap of this material can effectively be varied from 0–0.5 eV, allowing devices with operating wavelengths in the midwave infrared (MWIR) and long-wave infrared (LWIR) to be realized.

Several material systems have been demonstrated as effective MWIR LED devices. Interband quantum cascade (IQC) devices employing a multiple quantum well structure of InAs/GaInSb/AlSb emitting at 3.8 μm have been shown to reach output powers in excess of 400 μW from a $100 \times 100 \mu\text{m}^2$ mesa at room temperature with substrate thinning and surface texturing.² InAs based *p-i-n* diodes and double heterostructures based on InAsSb/InAsSbP have been investigated by Krier *et al.*^{3–5} At 3.8 μm , an output power of 2.1 mW was observed from a 300 μm diameter circular mesa using an InAsSb active region under pulsed current excitation.⁵ Liquid phase epitaxy grown AlGaAsSb/GaInAsSb/AlGaAsSb heterostructures have also been realized for high power MWIR LEDs. Output powers as high as 3.2 mW from a $500 \times 500 \mu\text{m}^2$ mesa under pulsed operating conditions emitting at 3.7 μm were demonstrated by Danilova *et al.*⁶ from a device with anisotropically etched sidewalls mounted in a parabolic reflector. Uncalibrated elec-

troluminescence from MWIR and LWIR InAs/GaSb SL devices has been observed previously.^{7,8}

Here, we demonstrate a strictly binary-binary SL design in a cascaded active region MWIR LED device. Use of the InAs/GaSb SL system permits a completely aluminum-free device structure, alleviating potential oxidation problems in mesa-processed diodes. By coupling N active regions via tunnel junctions, the I - V characteristics of the device can be scaled to accommodate the output characteristics of drive electronics. The turn on voltage of the diode will be $\sim E_g \times N$ depending on the tunnel junction design, where E_g is the SL band gap. The flexibility to adjust the device turn-on characteristics can be important when developing devices designed to work with drive electronics having low current supply capability but an appreciable voltage swing. Potential applications of such devices include gas sensing, IR communications, thermal imaging, process monitoring, and biomedical spectroscopy. In this configuration, the quantum efficiency of the device can theoretically be increased by a factor of N , as a given electron can radiatively recombine with a hole in each stage of the device.⁹ In practice the improvement will be less than a factor of N due, for example, to photon reabsorption in the doped tunnel junctions. Active region cascading also improves wallplug efficiency, as the effects of series resistance are reduced. Because cascading reduces the operating current by a factor of N , Joule heating due to series resistance can be reduced by a factor of N^2 .

SL LED devices were grown by molecular beam epitaxy (MBE) on Te doped GaSb (100) $\pm 0.1^\circ$ substrates. N -type substrates were used to reduce free carrier absorption, as the LEDs operate in a back emission geometry whereby the epise is bonded to a header and optical emission is collected through the substrate. The MBE system is equipped with arsenic and antimony valved cracker cells with cracking zones operated at 800 and 975 $^\circ\text{C}$, respectively. Under these conditions the arsenic population is expected to be largely As₂, and antimony composed of a mixture of Sb₂ and Sb monomers. Prior to growth, substrates were degreased in trichloroethylene as well as acetone and isopropanol, etched in HCl for 2 min to reduce the thickness of the native oxide

^{a)}Electronic mail: ekoerper@engineering.uiowa.edu.

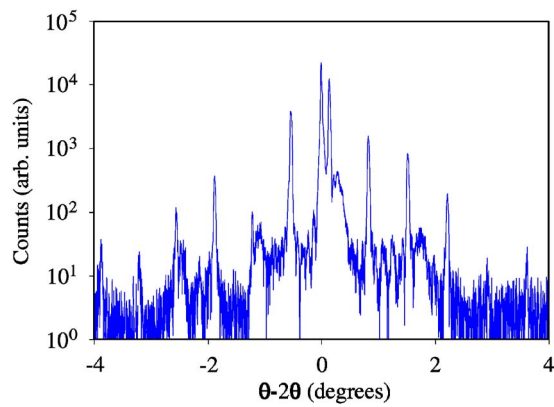


FIG. 1. (Color online) X-ray diffraction measurement of an eight stage cascaded LED structure. The strain is calculated to be 2.2×10^{-3} by a simulation of the structure and elastic theory considerations.

layer, rinsed with 2-propanol and blown dry with N_2 gas. Substrates were mounted in indium-free Mo wafer blocks with pyrolytic boron nitride diffusers in contact with the wafer for optimal heat distribution. After outgassing at 250°C for 1 h, substrates were loaded into the growth chamber, and the oxide was thermally desorbed at 530°C under Sb overpressure.

After thermal desorption, a thick $0.5\ \mu\text{m}$ n -type GaSb clad layer was grown at 500°C with a Te doping level of $1 \times 10^{18}\ \text{cm}^{-3}$. GaSb was grown at a rate of $0.55\ \text{ML/s}$ with a Sb/Ga beam equivalent pressure (BEP) ratio of 3:1 as measured with a nude ion gauge and InAs at a rate of $0.17\ \text{ML/s}$ with an As/In BEP ratio of 5:1. The substrate was then cooled to the SL growth temperature of 430°C as measured by an optical pyrometer referenced to the GaSb $(1 \times 3) \leftrightarrow (2 \times 5)$ surface reconstruction.¹⁰ A graded InAs/GaSb SL with constant GaSb thickness and increasing InAs content was then grown to smooth the conduction band energy so as to decrease the interfacial energy spike at the clad-SL interface. Each SL active region consists of 27 periods of 8.9 ML InAs/16 ML GaSb, for a total active region thickness of 200 nm. Tunnel junctions consisting of 50 nm p -type GaSb nominally Be doped to $5 \times 10^{18}\ \text{cm}^{-3}$ followed by a 45 nm thick graded n -type InAs/GaSb SL doped to $5 \times 10^{17}\ \text{cm}^{-3}$ couple the cascaded active regions. A third graded SL stack with decreasing InAs layer thickness and increasing GaSb thickness was used to avoid an interfacial spike in the valence band at the SL-GaSb cap interface. A 250 nm GaSb cap layer Be doped at $5 \times 10^{18}\ \text{cm}^{-3}$ completes the device. X-ray diffraction data of the cascaded LED in Fig. 1 show clearly defined SL peaks, and the strain, calculated by elastic theory, is 2.2×10^{-3} .

Wafers were processed into $120 \times 120\ \mu\text{m}^2$ mesa diodes by conventional wet etching and UV photolithography. Contacts of Ti/Pt/Au were applied to both anode and cathode by E-beam evaporation, and $1\ \mu\text{m}$ of indium was deposited by thermal evaporation. Processed devices were flip-chip bonded to GaAs headers. This method allows the epispide of the wafer to be in close thermal contact with the cooling system, separated only by the 0.5 mm thick GaAs header. It also eliminates the need to wire bond to the contact pads. Such a back-side-emission geometry is also beneficial in the sense that the mesa contact can act as a reflector and aid light extraction, and there is no metal contact obscuring the emission window.

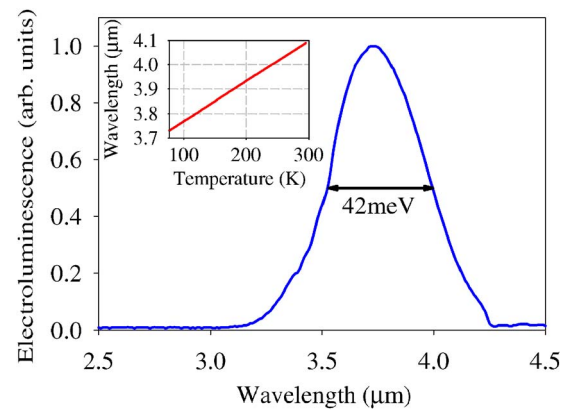


FIG. 2. (Color online) Electroluminescence from a $120 \times 120\ \mu\text{m}^2$ mesa diode operating at 77 K. The change in peak emission wavelength with temperature is shown in the inset.

Spectrally resolved electroluminescence is shown in Fig. 2, with the inset showing the temperature dependence of the peak emission wavelength. Calibrated temperature dependent measurements of LED emission were performed from room temperature to 77 K using a calibrated InSb detector cooled to 77 K and lock-in detection. Devices were biased with a voltage source operating at 500 Hz and 50% duty cycle. Optical emission was collected normal to the device surface without the use of a parabolic reflector, immersion lens, or integrating sphere. The emission distribution of the LEDs was measured to be that of a Lambertian source, allowing calculation of the axial power output. Total upper hemisphere power was then calculated by multiplying the axial power by π .

Plots of the total upper hemisphere emitted power versus drive current are shown in Fig. 3 for various temperatures. Devices turn on quickly for bias voltages exceeding 2.6 V, or about eight times the energy gap of the SL at 77 K, as expected for a $N=8$ stage device. This indicates that little extra voltage beyond $N \times E_g$ is required to turn on the device, suggesting that the tunnel junctions are working well. At 77 K, output power exceeding $700\ \mu\text{W}$ was achieved at 20 mA drive current, and output of approximately 1.5 mW was measured at 100 mA. For operation at 77 K, no further increase in emission is observed beyond 120 mA drive current. At this point, $\sim 400\ \text{mW}$ of electrical power is being

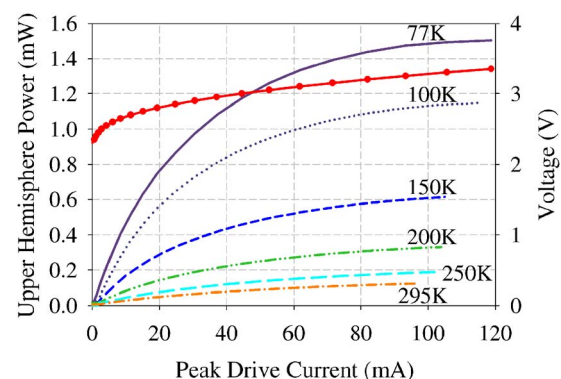


FIG. 3. (Color online) Calibrated output power as a function of current ($L-I$ curves) at various temperatures. Devices are believed to be thermally limited, as evidenced by the decrease in the slope of the $L-I$ curves after 10 mA. The 77 K $I-V$ characteristic (dotted red curve) is associated with the right side axis.

dissipated in the device. We attribute this roll off in output power in part to heating of the active regions due to the quasi-dc nature of the current injection and the small size of the device. Hole leakage is also expected to cause quenching of optical output due to limited carrier confinement.

To place the performance of the SL LEDs in context with that of existing technologies for MWIR emitters, we compare our results with published data for similar IQC LEDs. Output from nine-stage IQC LEDs has been reported by Das *et al.* to reach nearly 140 μW for a 100 μm mesa and 180 μW for a 150 μm mesa at room temperature,¹¹ but only after removing essentially all the substrate and applying a linear grating on the output surface to enhance the extraction efficiency (see Fig. 5 in Ref. 11). These results are from LEDs with a comparable number of cascaded stages and with mesa sizes slightly smaller and slightly larger than those reported here. Comparison of these data indicates that our SL LED and the IQC devices produce comparable output power at room temperature. A comparison at cryogenic temperatures can be made by noting that Das *et al.* report a factor of 5.3 increase in output power as the IQC LED temperature is decreased from room temperature to 77 K. Again, based on the data in Fig. 5 of Ref. 11, at 77 K one would observe approximately 740 and 950 μW from the 100 and 150 μm IQC mesas, respectively. In contrast, we measure up to 1.5 mW of output power at 77 K from our eight-stage SL LED using a 120 μm mesa. This is twice the power of the 100 μm IQC device and roughly 60% more power than the larger 150 μm IQC device. We emphasize that the IQC devices used for this comparison incorporated one more stage than was used for the SL LED, the IQC substrate was essentially removed, and an output enhancing grating was applied to the IQC. If similar power enhancement approaches were applied to the SL LED, we would expect roughly a factor of

two increase in output power, i.e., a maximum of 3 mW at 77 K.

In conclusion, we have demonstrated optically efficient cascaded active region, InAs/GaSb SL LEDs with a completely aluminum-free design for MWIR emission. Without making any attempt to enhance extraction efficiency, e.g., by thinning the substrate or texturing the output surface, output powers as high as 1.5 mW at 77 K have been observed from $120 \times 120 \mu\text{m}^2$ mesa diodes biased at 3.2 V with 100 mA peak drive current. The results suggest that, while these SL LEDs can provide performance comparable to that reported for IQC LEDs at room temperature, they are superior to the IQC devices at cryogenic temperatures.

The authors would like to thank the Test Resource Management Center (TRMC) Test and Evaluation/Science and Technology (T&E/S&T) Program for their support. This work is funded by the T&E/S&T Program through the University of Iowa Contract No. W91ZLK-06-C-0006.

¹L. Esaki and R. Tsu, *IBM J. Res. Dev.* **14**, 61 (1970).

²N. C. Das, *Appl. Phys. Lett.* **90**, 011111 (2007).

³A. Krier and M. Fisher, *IEE Proc.: Optoelectron.* **144**, 287 (1997).

⁴A. Krier and V. Sherstnev, *J. Phys. D* **33**, 101 (2000).

⁵A. Krier, V. Sherstnev, and H. Gao, *J. Phys. D* **33**, 1656 (2000).

⁶T. Danilova, B. Zhurtanov, A. Imenkov, and Y. P. Yakovlev, *Semiconductors* **39**, 1281 (2005).

⁷D. Hoffman, A. Hood, E. Michel, F. Fuchs, and M. Razeghi, *IEEE J. Quantum Electron.* **42**, 126 (2006).

⁸D. Hoffman, A. Gin, Y. Wei, A. Hood, F. Fuchs, and M. Razeghi, *IEEE J. Quantum Electron.* **41**, 1474 (2005).

⁹B. H. Yang, D. Zhang, R. Q. Yang, C.-H. Lin, S. J. Murry, and S. S. Pei, *Appl. Phys. Lett.* **72**, 2220 (1998).

¹⁰A. Bracker, M. Yang, B. Bennett, J. Culbertson, and J. Moore, *J. Cryst. Growth* **220**, 384 (2000).

¹¹N. C. Das, K. Olver, and F. Towner, *Solid-State Electron.* **49**, 1422 (2005).